BASIC RESEARCH www.jasn.org

# Small-Molecule CFTR Inhibitors Slow Cyst Growth in Polycystic Kidney Disease

Baoxue Yang,* Nitin D. Sonawane,* Dan Zhao,* Stefan Somlo,† and A. S. Verkman*

*Departments of Medicine and Physiology, University of California, San Francisco, California; and †Department of Internal Medicine, School of Medicine, Yale University, New Haven, Connecticut

## ABSTRACT

Cyst expansion in polycystic kidney disease (PKD) involves progressive fluid accumulation, which is believed to require chloride transport by the cystic fibrosis transmembrane conductance regulator (CFTR) protein. Herein is reported that small-molecule CFTR inhibitors of the thiazolidinone and glycine hydrazide classes slow cyst expansion in *in vitro* and *in vivo* models of PKD. More than 30 CFTR inhibitor analogs were screened in an MDCK cell model, and near-complete suppression of cyst growth was found by tetrazolo-$CFTR_{inh}$-172, a tetrazolo-derived thiazolidinone, and Ph-GlyH-101, a phenyl-derived glycine hydrazide, without an effect on cell proliferation. These compounds also inhibited cyst number and growth by >80% in an embryonic kidney cyst model involving 4-d organ culture of embryonic day 13.5 mouse kidneys in 8-Br-cAMP–containing medium. Subcutaneous delivery of tetrazolo-$CFTR_{inh}$-172 and Ph-GlyH-101 to neonatal, kidney-specific PKD1 knockout mice produced stable, therapeutic inhibitor concentrations of >3 $\mu$M in urine and kidney tissue. Treatment of mice for up to 7 d remarkably slowed kidney enlargement and cyst expansion and preserved renal function. These results implicate CFTR in renal cyst growth and suggest that CFTR inhibitors may hold therapeutic potential to reduce cyst growth in PKD.

*J Am Soc Nephrol* 19: 1300–1310, 2008. doi: 10.1681/ASN.2007070828

Polycystic kidney disease (PKD) is characterized by massive enlargement of fluid-filled cysts of renal tubular origin that compromise normal renal parenchyma and cause renal failure.[1–6] Human autosomal dominant PKD (ADPKD) is caused by mutations in one of two genes, *PKD1* and *PKD2*, encoding the interacting proteins polycystin-1 and polycystin-2, respectively.[4,7–10] Cyst growth in PKD requires fluid secretion into the cyst lumen coupled with epithelial cell hyperplasia.

*In vitro* data implicate epithelial chloride secretion in generating and maintaining fluid-filled cysts.[11–14] The cystic fibrosis transmembrane conductance regulator protein (CFTR), a cAMP-regulated chloride channel, is believed to provide the principal route for chloride entry into expanding cysts. CFTR is expressed in the apical membrane of cyst-lining epithelial cells in PKD kidneys.[13,15] A CFTR inhibitor discovered by our laboratory, $CFTR_{inh}$-172,[16] has been shown to slow cyst growth in an MDCK cell culture model of PKD[14] and in metanephric kidney organ cultures.[17] In families affected with both ADPKD and cystic fibrosis, individuals with both ADPKD and cystic fibrosis had less severe renal disease than those with only ADPKD.[18,19] These findings provide a rational basis for evaluation of CFTR inhibitors in ADPKD therapy.

We have identified, by high-throughput screening, two types of CFTR inhibitors that block, by different mechanisms, CFTR chloride channel

Received July 28, 2007. Accepted January 17, 2008.

Published online ahead of print. Publication date available at www.jasn.org.

**Correspondence:** Dr. A. S. Verkman, 1246 Health Sciences East Tower, Cardiovascular Research Institute, University of California, San Francisco, San Francisco, CA 94143-0521. Phone: 415-476-8530; Fax: 415-665-3847; E-mail: alan.verkman@ucsf.edu

function. $CFTR_{inh}$-172 is a thiazolidinone that reversibly inhibits CFTR $Cl^-$ channel function[16] (Figure 1). Patch-clamp analysis indicated that $CFTR_{inh}$-172 stabilizes the channel's closed state, probably by binding to a cytoplasmic domain of CFTR.[20] After intravenous bolus infusion in rodents, $CFTR_{inh}$-172 was concentrated in the kidney and urine with respect to blood and was excreted with little metabolism.[21] The glycine hydrazides (*e.g.*, GlyH-101; Figure 1) bind directly to the CFTR pore at a site near its external entrance.[22] We synthesized membrane-impermeable GlyH-101 analogs, including conjugates to polyethylene glycols[23] and lectins,[24] that block CFTR $Cl^-$ current from the cell exterior.

Here, we evaluated and optimized CFTR inhibitors for PKD therapy. We screened a panel of thiazolidinones and glycine hydrazides with improved properties over $CFTR_{inh}$-172 and GlyH-101 for their efficacy in inhibiting cyst growth in an *in vitro* MDCK cell model. The best compounds were then tested in an embryonic kidney organ culture model and *in vivo* using a *Pkd1*$^{flox/-}$*;Ksp-Cre* mouse model of postnatal ADPKD.

## RESULTS

### CFTR Inhibitors Reduce Cyst Formation and Growth in an MDCK Cell Cyst Model

An MDCK cell model of PKD was used to screen 32 CFTR inhibitors of the thiazolidinone and glycine hydrazide classes for reducing cyst formation and expansion. Cells were cultured in a collagen matrix containing 10 $\mu$M forskolin. Cysts were seen at 3 to 4 d, progressively enlarging during the next 8 d (Figure 2A, top). Cysts did not form in the absence of forskolin (data not shown). Exposure of established cysts (>50 $\mu$m in diameter on day 4) to a CFTR inhibitor (compound T08) at 10 $\mu$M for 8 d slowed cyst enlargement (Figure 2A, middle). Inhibition was reversible as shown by exposure to inhibitor at days 4 through 8 followed by washout (Figure 2A, bottom).

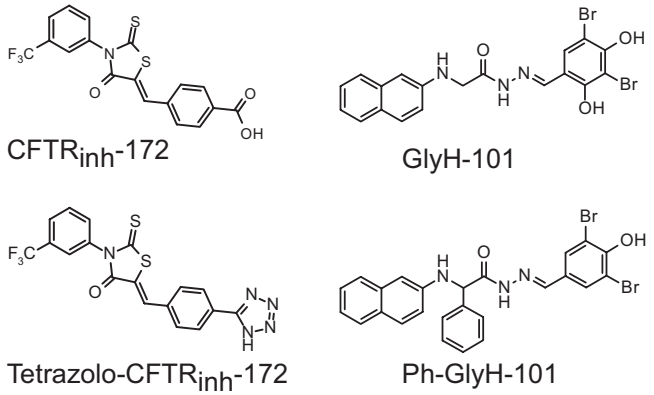


**Figure 1.** Structures of CFTR inhibitors. Chemical structures of $CFTR_{inh}$-172 (thiazolidinone class) and GlyH-101 (glycine hydrazide class). Shown also are analogs tetrazolo-$CFTR_{inh}$-172 and Ph-GlyH-101, which had best properties for inhibition of renal cyst expansion.

Thirty-two CFTR inhibitors (at 10 $\mu$M) were screened in the MDCK cell model. Compound structures together with their approximate CFTR inhibition potencies (expressed as IC50 values) are provided in Figures 3 and 4. Eight compounds inhibited cyst growth by >70% (Figure 2B). For testing whether inhibition of cyst growth could be related to cytotoxicity, cell viability was assayed by crystal violet staining. At 20 $\mu$M, compounds T09, T12, T13, G04, and G05 reduced MDCK cell viability, whereas compounds T08, T14, G03, G07, and G16 did not (Figure 2C).

Cyst growth was measured from days 4 through 12 with compounds T08, T14, G07, and G16 at 1, 5, and 10 $\mu$M. Compounds G07 (a glycine hydrazide analog) and T08 (a thiazolidinone analog) strongly inhibited cyst enlargement at 1 $\mu$M (Figure 2D).

For examination of effects on cyst formation, MDCK cells were incubated from day 0 with compounds (at 10 $\mu$M) in the presence of forskolin. On day 6, we counted spherical cysts (with diameter >50 $\mu$m) and noncyst cell colonies. Figure 2E shows that the total numbers of colonies (cysts plus noncyst colonies) were similar in the control and inhibitor-treated groups. Compounds T08, T14, G07, and G16 greatly reduced the number of cysts. $CFTR_{inh}$-172 also inhibited cyst formation but to a lesser extent. Compounds T08 and G07, representing the most potent (and nontoxic) compounds of the glycine hydrazide and thiazolidinone classes, respectively, were further evaluated.

CFTR inhibition potency was confirmed in MDCK cells by short-circuit current analysis. Figure 2F shows the concentration-dependent inhibition of short-circuit current after CFTR simulation by forskolin, with IC50 of approximately 1 $\mu$M.

Compounds T08 and G07 were tested in cell proliferation and apoptosis assays. Figure 2G shows that at 10 $\mu$M, these compounds did not inhibit MDCK cell proliferation or cause apoptosis. Figure 2H shows that these compounds did not alter CFTR expression as seen by similar short-circuit current in MDCK cells after 1 *versus* 48 h of incubation with 10 $\mu$M T08 or G07 followed by washout.

### CFTR Inhibitors Retard Cyst Development and Growth in Embryonic Kidney Culture

An embryonic kidney organ culture model was used to evaluate further compounds T08 and G07. Embryonic kidneys from wild-type embryonic day 13.5 (E13.5) mice were cultured for 4 d in the absence or presence of 100 $\mu$M 8-Br-cAMP. In the absence of 8-Br-cAMP, kidneys increased in size over 4 d (Figure 5A, top), whereas numerous cystic structures were seen in the presence of 8-Br-cAMP (Figure 5A, bottom). Figure 5B shows that compounds T08 and G07 remarkably reduced cyst formation, as confirmed by quantitative image analysis (Figure 5C). In control studies, cysts formed after compound washout after 2-d treatment (Figure 5D, top), indicating reversible action of CFTR inhibitors. Also, kidney growth in the absence of 8-Br-cAMP was not affected by the CFTR inhibitors. After 4 d in culture,

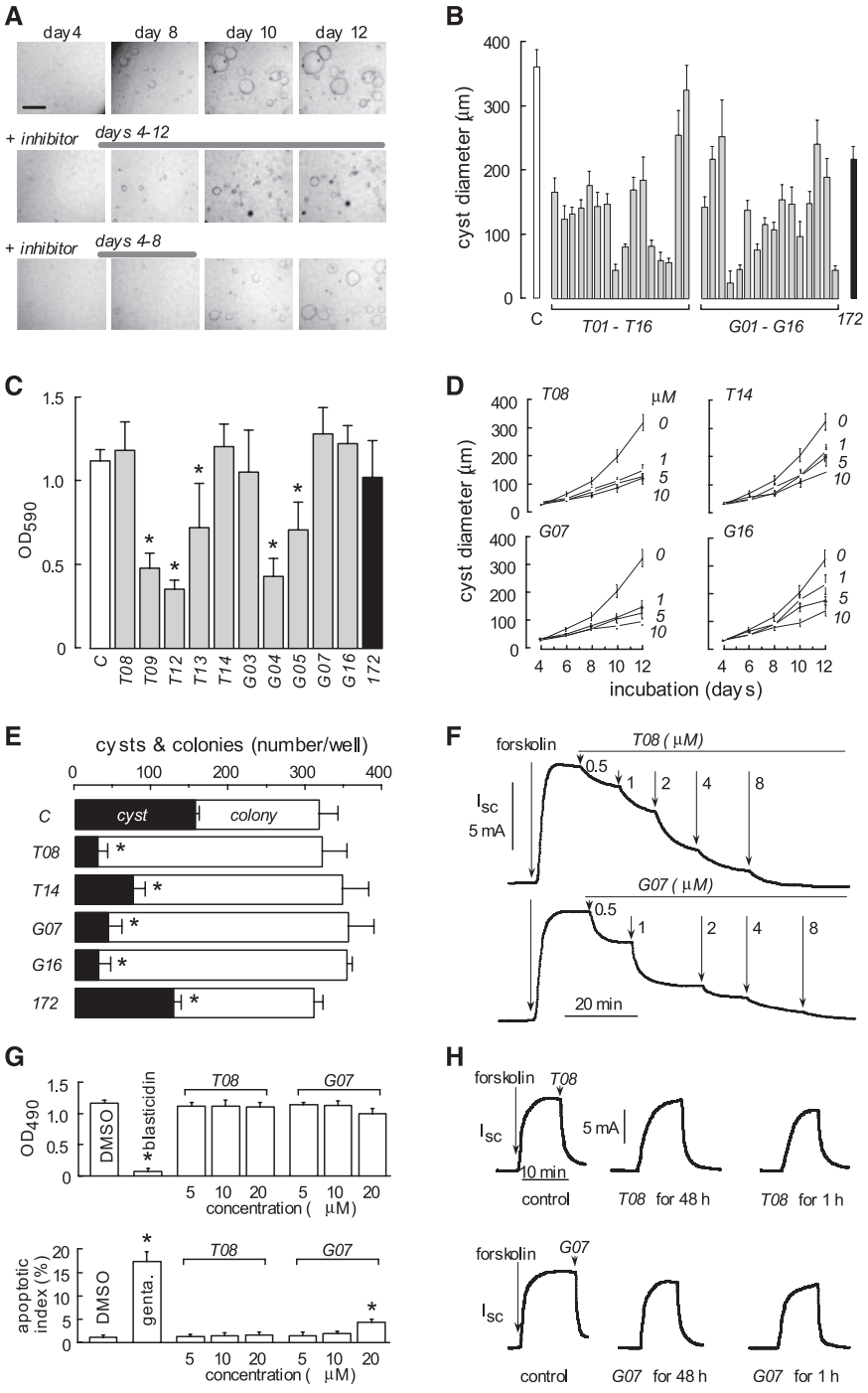


**Figure 2.** CFTR inhibitors slow growth of MDCK cell cysts in cell culture. (A) Representative light micrographs of MDCK cell cyst growth in collagen gels. Light micrographs taken at indicated days after cell seeding of MDCK cells exposed continuously to 10 $\mu$M forskolin (top). In some experiments, CFTR inhibitor T08 was added for 8 d (middle) or 4 d (bottom), from day 4 onward after cell seeding in gels. Bar = 500 $\mu$m. (B) Cyst inhibition activity of thiazolidinone and glycine hydrazide analogs T1 through T16 and G1 through G16 (SE, $n > 10$). C, DMSO vehicle control; 172, $CFTR_{inh}$-172. (C) Cytotoxicity assayed by crystal violet staining (SE, $n = 3$, $^*P < 0.05$). (D) MDCK cell cyst growth shown as cyst diameters for indicated compounds (SE, $n > 30$ cysts analyzed per time point). (E) MDCK cell cyst formation. □, Total numbers of colonies (including cysts and noncyst colonies) per well on day 6 after MDCK cell seeding in the absence (control) and presence of test compounds (at 10 $\mu$M); ■, numbers of cysts with diameter >50 $\mu$m (SE, four wells per condition, $^*P < 0.05$). (F) Inhibition of short-circuit current in MDCK cell monolayer by compounds T08 and G07 after chloride current stimulation by 20 $\mu$M forskolin. (G, top) MDCK cell proliferation measured by BrdU incorporation (SE, $n = 3$, $^*P < 0.05$). Where indicated, T08 or G07 was present in the medium for 72 h. DMSO was used as negative control. Blasticidin (20 $\mu$g/ml) was used as positive control. (Bottom) MDCK cell apoptosis assayed by the detection of fluorescein-dUTP–labeled DNA strand breaks by fluorescence microscopy (SE, $n = 5$, $^*P < 0.05$). Where indicated, T08 or G07 was present in medium for 72 h. DMSO was used as negative control. Gentamicin (2 mM) was used as positive control. (H) Short-circuit current in MDCK cell monolayers cultured without or with 10 $\mu$M T08 or G07 for 1 or 48 h. Compounds were washed out for 1 h before measurements. CFTR chloride current was stimulated by 20 $\mu$M forskolin.

kidney lengths were 1.48 ± 0.10 (T08-treated), 1.42 ± 0.08 (G07-treated) and 1.46 ± 0.08 mm (control).

Paraffin sections are shown in Figure 5E. In the absence of 8-Br-cAMP, after 4 d in culture, renal tubules and primitive distal ramifications of the ureteric bud formed. Large cystic structures were seen throughout the kidney in the presence of 8-Br-cAMP. Compounds T08 and G07 reduced the number and size of cysts. The apoptotic index was <1% in kidneys exposed to T08 or G07 at 20 $\mu$M (data not shown).

## CFTR Inhibitors Slow Cyst Development in a $Pkd1^{flox/-}$;Ksp-Cre Mouse Model of ADPKD

Mass spectrometry was used to assay compound concentration in urine and kidney homogenates. Representative HPLC and mass chromatograms are provided in Figure 6A, showing 50-pM sensitivity. Tetrazolo-$CFTR_{inh}$-172 (compound T08) and Ph-GlyH-101 (compound G07) were detected by absorbance at 386 and 338 nm, respectively, with mass traces of m/z 433.4 Da and 553.2 Da. Assays were linear over 0.05 to 15 $\mu$g/ml, with 0.01 $\mu$g/ml detection limit. Assay sensitivity and specificity were confirmed by addition of known quantities of inhibitors to urine from non–compound-treated mice (Figure 6B).

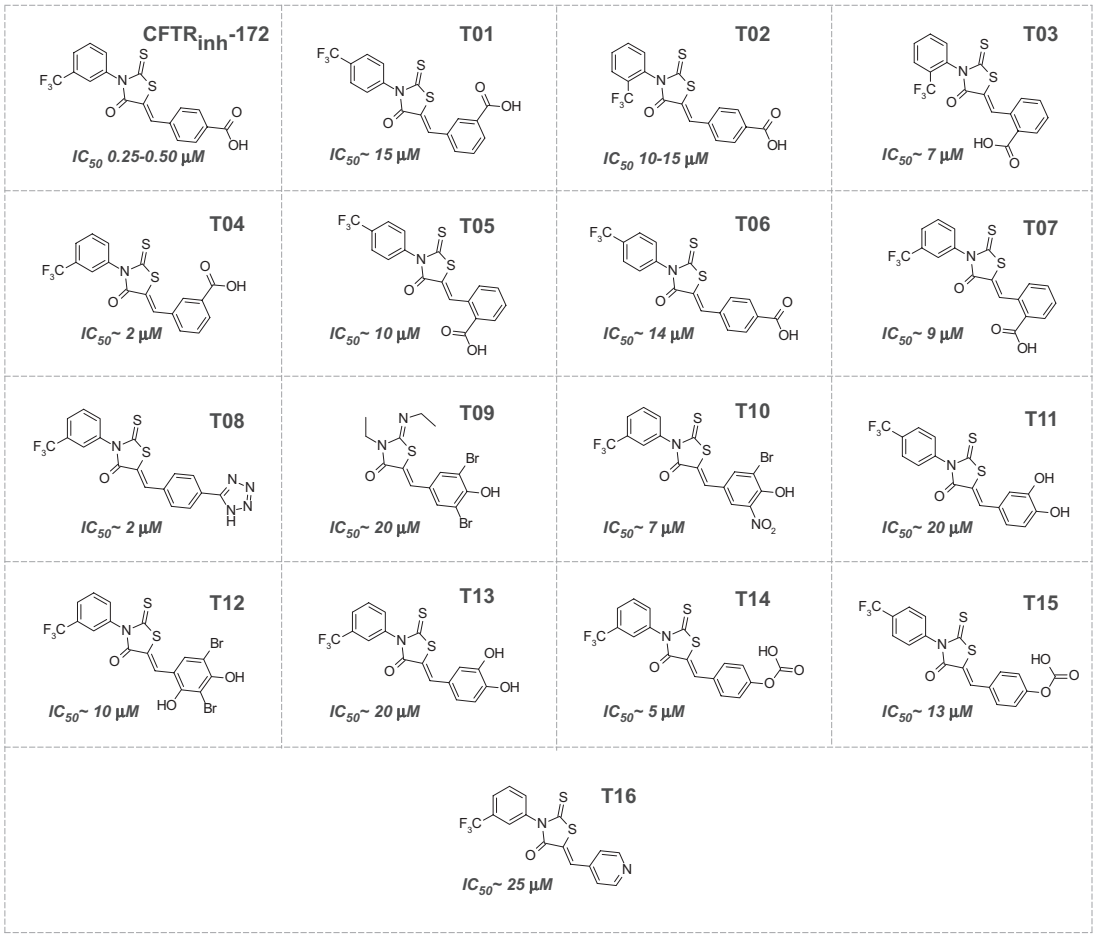


**Figure 3.** Structures of thiazolidinone CFTR inhibitors with their CFTR inhibition activity. IC50 values for T01 through T07, T10, and T12 through T14 were as reported.[16] IC50 for T08, T11, and T16 were determined by short-circuit analysis.

Concentrations were measured to establish dosing to give sustained concentrations in kidney/urine of $>1$ $\mu$M, where CFTR is inhibited. Kidney and urine samples were obtained from mice after 4-times-daily subcutaneous administration for 3 d at 5 mg/kg per d, a dosage regimen determined from preliminary studies. Urinary concentrations were measured at 1 and 5 h after the final dosing. For tetrazolo-$CFTR_{inh}$-172, urine concentrations were 3.3 and 3.6 $\mu$M at 1 and 5 h, respectively. The urine concentrations of Ph-GlyH-101 were 4.3 and 5.8 $\mu$M. Comparable inhibitor concentrations were found in kidney homogenates. These concentrations are several-fold greater than the IC50 for CFTR inhibition.

For *in vivo* studies, we used kidney-specific Pkd1 knockout mice (*Pkd1*$^{flox/-}$*;Ksp-Cre*) generated by breeding *Pkd1*$^{flox/flox}$ mice with *Pkd1*$^{+/-}$*;Ksp-Cre* mice. *Pkd1*$^{flox/-}$*;Ksp-Cre* mice develop rapidly, progressive cysts in the neonatal period, resulting in renal failure and death by age 20 d.[25] Effective CFTR inhibitory concentrations in kidney/urine were obtained by subcutaneous compound administration at 5 to 10 mg/kg per d every 6 h from days 2 through 5. Control *Pkd1*$^{flox/-}$*;Ksp-Cre* mice received DMSO vehicle alone. *Pkd1*$^{flox/+}$*;Ksp-Cre* or *Pkd1*$^{flox/-}$ and *Pkd1*$^{flox/+}$ mice from the same litter (these non-PKD mice are referred to as "wild-type") were studied for comparison. During the treatment period, control and *Pkd1*$^{flox/-}$*;Ksp-Cre* mice, with or without CFTR inhibitor treatment, were indistinguishable in their activity and behavior. After 3 d of treatment (age 5 d), there was no difference in body weight in any of the mouse groups (data not shown).

Figure 7A shows central coronal kidney sections. Although there was considerable mouse-to-mouse variability, kidney sections from T08- and G07-treated mice showed fewer cysts of all sizes. Kidney weights in T08- and G07-treated wild-type mice were similar to those in untreated control mice (Figure 7B). Kidney weight in *Pkd1*$^{flox/-}$*;Ksp-Cre* mice was more than three-fold higher than in wild-type mice. Treatment of *Pkd1*$^{flox/-}$*;Ksp-Cre* mice with compounds T08 or G07 reduced kidney weight significantly compared with vehicle-treated *Pkd1*$^{flox/-}$*;Ksp-Cre* mice. Image analysis of hematoxylin- and eosin-stained sections showed remarkably fewer total numbers of cysts (of $>50$ $\mu$m in diameter) per kidney in T08- and G07-treated mice (797 $\pm$ 69, control; 457 $\pm$ 32, T08; 316 $\pm$ 45, G07), with reduced numbers of medium- and large-size cysts (Figure 7C).

Another group of mice was treated with T08 and G07 for 7 d

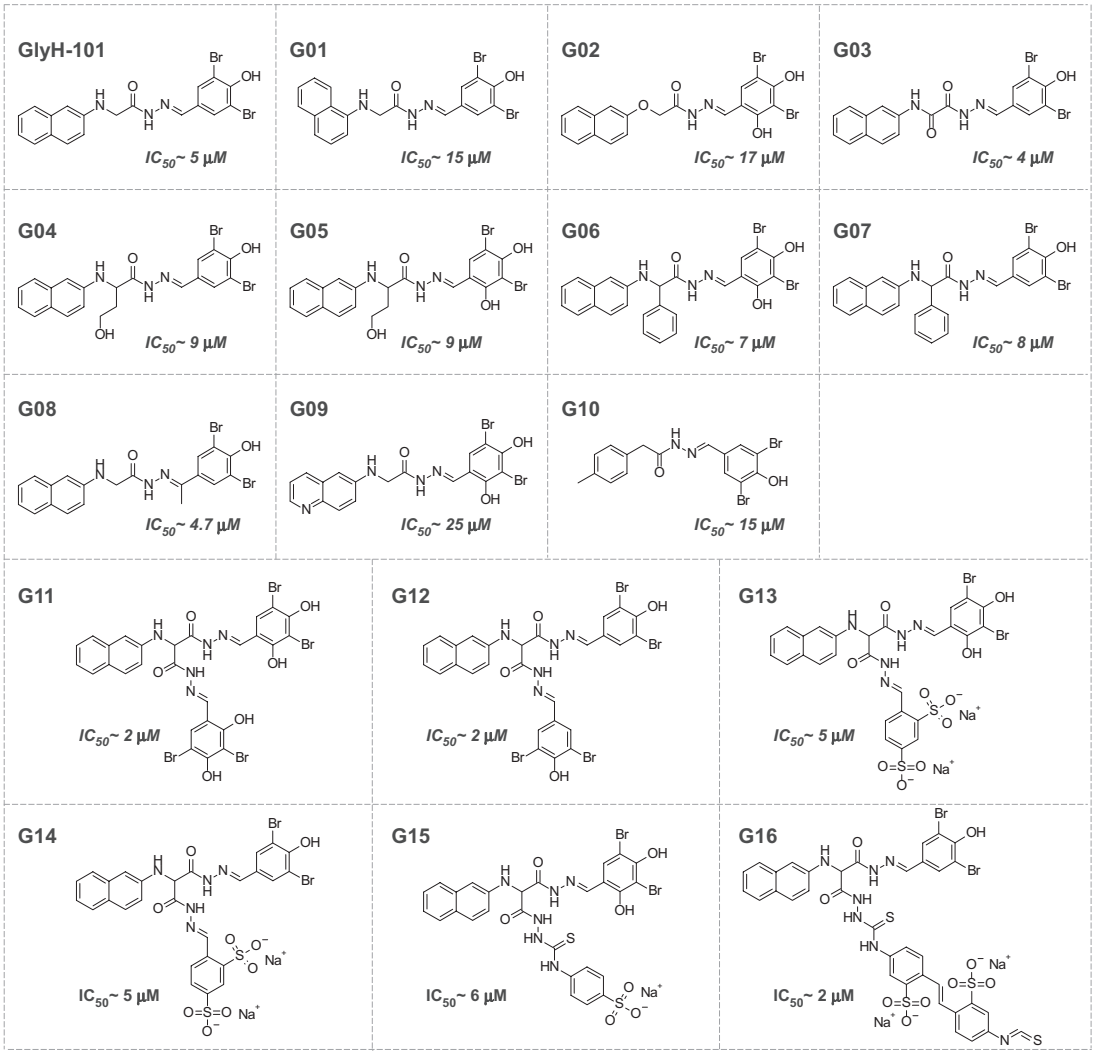


**Figure 4.** Structures of glycine hydrazide and malonic acid hydrazide CFTR inhibitors with their CFTR inhibition activity. IC50 values for G01 through G05 and G8 through G16 were as reported.[23,24] IC50 for G06 and G07 were determined by short-circuit current analysis.

("day 9" kidneys), when significant reduction in renal function was found in untreated *Pkd1*$^{flox/-}$*;Ksp-Cre* mice. Figure 7D shows mild elevations in serum creatinine and urea in vehicle-treated *Pkd1*$^{flox/-}$*;Ksp-Cre* mice (compared with wild-type mice) at 3 d ("day 5" kidneys), with more marked elevations at day 9. Serum creatinine and urea were significantly reduced in T08- and G07-treated *Pkd1*$^{flox/-}$*;Ksp-Cre* mice, although not as low as in wild-type mice.

## DISCUSSION

The goals of this study were to establish the efficacy of small-molecule CFTR inhibitors to retard cyst expansion in PKD and to select the best thiazolidinone- and glycine hydrazide–class CFTR inhibitors. We used three distinct experimental models of cystic kidney disease to obtain proof of concept for small-molecule CFTR inhibitors for therapy of PKD. Screening of 32 thiazolidinone and glycine hydrazide analogs in MDCK cell culture identified compounds that strongly reduced cyst number and growth, without toxicity or inhibition of cell proliferation. The best compounds had low micromolar potency and were effective in inhibiting cyst growth in embryonic kidney organ cultures. After establishing conditions for compound administration to neonatal mice to achieve "therapeutic" concentrations in kidneys and urine, the best CFTR inhibitors partially inhibited cyst growth and preserved renal function in a mouse model of ADPKD.

cAMP signaling plays an important role in renal cyst development.[26–28] Cyst growth in PKD involves fluid secretion into the cyst lumen coupled with epithelial cell hyperplasia.[29,30] As described at the beginning of this article, *in vitro* data implicate epithelial chloride secretion in the generation and maintenance of fluid-filled cysts.[11–14] As in other secretory epithelia, fluid secretion into the cyst lumen occurs by primary chloride exit across the cell apical mem-

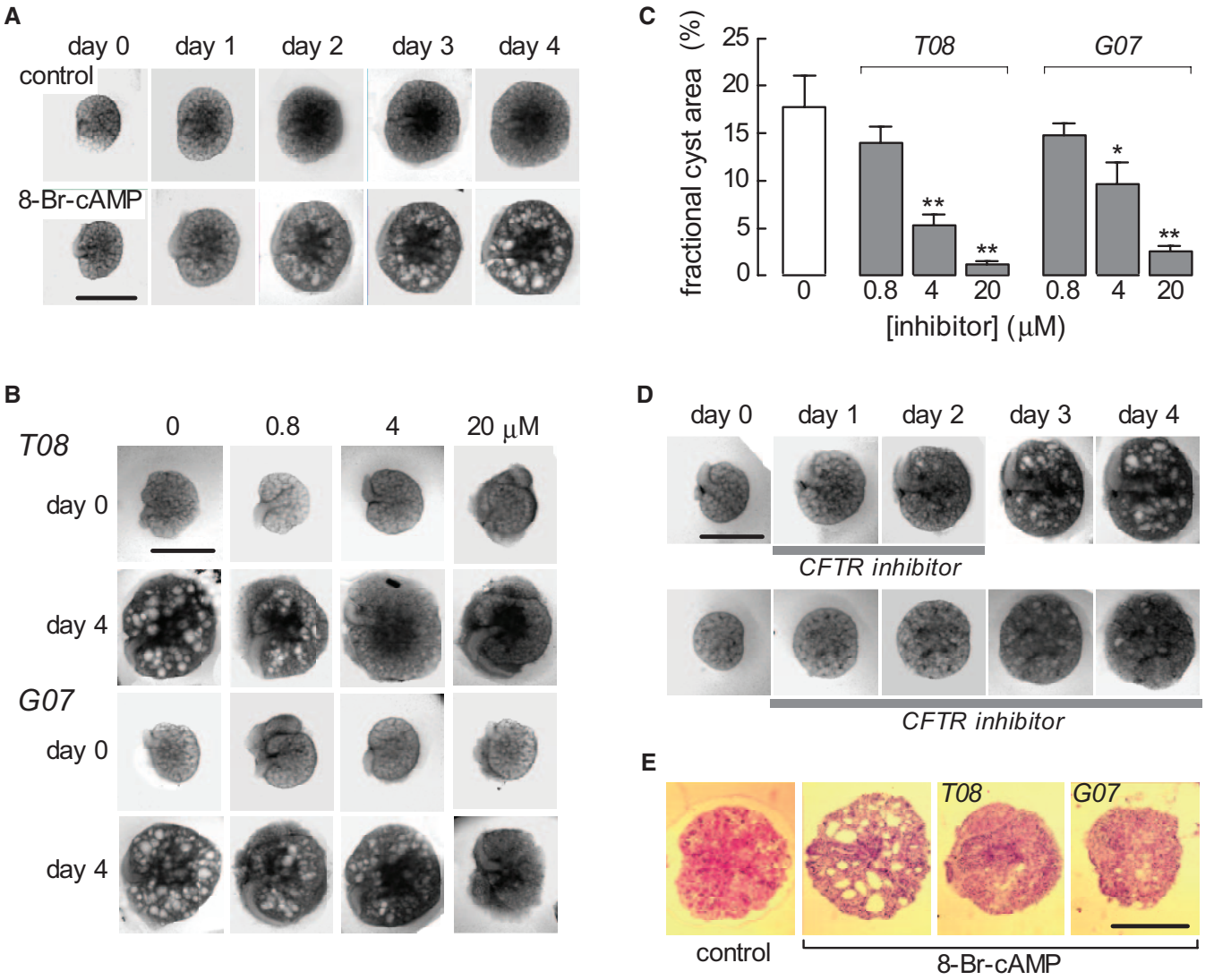


**Figure 5.** CFTR inhibitors slow cyst growth in embryonic kidney organ cultures. Embryonic kidneys were placed in culture at day E13.5 and maintained for 4 d. (A) Kidney appearance by transmitted light microscopy for cultures in the absence (top) or continued presence (bottom) of 100 $\mu$M 8-Br-cAMP. Each series of photographs shows the same kidney on successive days in culture. Bar = 1 mm. (B) Inhibition of cAMP-induced cyst growth by compounds T08 and G07. Images shown of embryonic kidneys before (day 0) and 4 d after compound addition. Bar = 1 mm. (C) Fractional cyst area in control and CFTR inhibitor–treated kidneys (SE, $n = 6$ to 12, $^*P < 0.05$, $^{**}P < 0.01$ *versus* control). (D) Reversible inhibition of cyst growth. Compound T08 was added for 2 d (top) or 4 d (bottom) in culture medium containing 100 $\mu$M 8-Br cAMP. Bar = 1 mm. (E) Histology (hematoxylin and eosin staining) of embryonic kidneys. Bar = 1 mm.

brane, which secondarily drives transepithelial sodium and water secretion. Lumenal fluid accumulation causes progressive cyst expansion directly by net water influx into the cyst lumen and indirectly by stretching cyst wall epithelial cells to promote their division and thinning.[11,13,31] CFTR inhibition interferes with fluid secretion at the apical chloride exit step.

MDCK type I cells, which endogenously express CFTR,[32] provide a useful *in vitro* model of cystogenesis for screening of candidate inhibitors of cyst formation and growth. Culture of MDCK cells in three-dimensional collagen gels produces a polarized, single-layer, thinned epithelium surrounding a fluid-filled space, apical external-facing microvilli, a solitary cilium, and apical tight junctions.[33–35] MDCK cells in cysts undergo proliferation, fluid transport, and matrix remodeling, as seen in tubular epithelial cells cultured from PKD kidneys. Cyst formation and growth are cAMP dependent, which is thought to increase independently cell proliferation and activate CFTR-facilitated transepithelial fluid secretion.[26–31] Recognizing its limitations, such as differences between MDCK *versus* renal epithelial cells and cell cultures *versus* intact kidneys, the MDCK cyst model identified CFTR inhibitors that reduced cyst formation and enlargement without demonstrable cell toxicity or inhibition of cell proliferation.

The embryonic kidney culture model permits organotypic

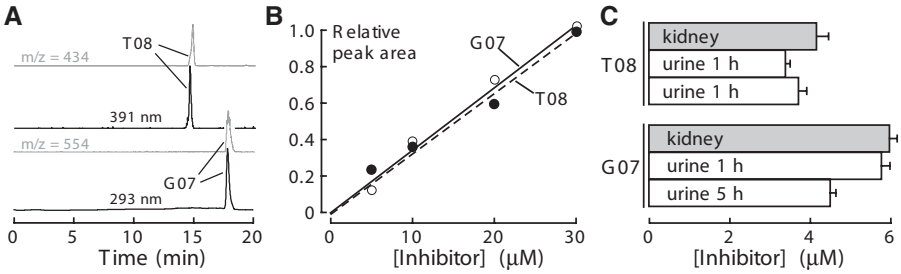


**Figure 6.** Liquid chromatography/mass spectrometry analysis of inhibitor concentrations in kidney and urine. (A) Representative HPLC profile of urine spiked with 50 pM each of tetrazolo-$CFTR_{inh}$-172 (compound T08, top) and Ph-GlyH-101 (compound G07, bottom) with their respective mass trace profiles of 432 *m/z* (top inset) and 554 *m/z* (bottom inset), demonstrating assay sensitivity. (*B*) Calibrations of absorbance peak areas (from HPLC) for known amounts of inhibitors added to urine. (C) Urine concentrations at 1 and 5 h after subcutaneous administration at 5 to 10 mg/kg per d for 3 d (SE, $n = 3$).

growth and differentiation of renal tissue in defined media without the confounding effects of circulating hormones and glomerular filtration.[17,36] In metanephric organ culture, the early mouse kidney tubule has an intrinsic capacity to secrete fluid in response to cAMP by a CFTR-dependent mechanism.[17] The CFTR inhibitors T08 and G07 reversibly inhibited cyst formation and growth in embryonic kidneys. Although embryonic kidney cultures probably represent a better PKD model than MDCK cells, they are avascular and nonperfused and therefore are not exposed to the same environment as *in vivo* kidney.

We used *Pkd1*$^{flox/-}$*;Ksp-Cre* mice, which are kidney-selective *Pkd1* knockout mice that manifest a fulminant course, with development of large cysts and renal failure in the first 2 wk of life and death by 20 d. This model is suitable to evaluate the efficacy of CFTR inhibitors on retarding the growth of cysts in the distal segments of the nephron, including medullary thick ascending limbs of the loops of Henle, distal convoluted tubule, and collecting ducts.[37] In humans, ADPKD develops slowly and causes renal failure at an average age >50 yr. For these studies, we chose to use this relatively severe model of ADPKD, rather than mouse models that develop disease more slowly, because of the shorter time required for compound administration and the greater likelihood of observing an immediate benefit. Testing of small-molecule CFTR inhibitors in ADPKD mouse models with slower onset should be of further utility in predicting efficacy in human ADPKD. The CFTR inhibitors significantly reduced cyst formation and clinical signs of PKD, as assessed by lower kidney weights, and serum creatinine and urea concentrations.

The ideal properties of a CFTR inhibitor for therapy of PKD include high potency and CFTR specificity, low toxicity, concentration in kidney and urine, and suitability for chronic oral administration. A limitation of the thiazolidinone $CFTR_{inh}$-172 has been its high lipophilicity (logP 4.26 calculated by ChemAxon) and relatively low solubility of approximately 17 $\mu$M in saline, associated with precipitation, particularly in acidic solutions, and adsorption to surfaces. We synthesized close $CFTR_{inh}$-172 analogs by changing positions of trifluoromethyl and carboxy substitutes to effect reduction in lattice energy (compounds T01 through T07) and replacing carboxy group by isoster tetrazolo (T08), hydroxyl (T09 through T13), and carboxyoxy (T14 through T16) functions. These compounds showed good CFTR inhibition, with tetrazolo-$CFTR_{inh}$-172 (T08) having good aqueous solubility (190 $\mu$M in saline). Of the GlyH-101 analogs, we evaluated a variety of compounds already synthesized[22,23] with varied solubility, polarity, and potency (compounds G01 through G16). The best compound found in this class was the phenyl-derived analog Ph-GlyH-101, which was more lipophilic than GlyH-101 (logP, 7.11 *versus* 5.14) and thus likely to have greater systemic absorption and oral bioavailability. Because this study was focused on proof of concept for use of CFTR inhibitors in PKD models, we did not carry out more extensive analysis of *in vivo* pharmacology and toxicity, as would be necessary for further preclinical development.

The data here indicate that thiazolidinone- and glycine hydrazide–type small-molecule CFTR inhibitors, at concentrations without apparent toxicity or inhibition of cell proliferation, retarded the growth of renal cysts in *in vitro* and *in vivo* PKD models. Our data support the conclusion that CFTR-dependent fluid secretion is an important determinant in the development and growth of renal epithelial cell cysts. Antisecretory therapy for PKD would provide an alternative strategy to antiproliferative therapies. Development of cystic fibrosis–like lung disease is unlikely with long-term CFTR inhibitor treatment because of minimal CFTR inhibitor accumulation in lung[21] and the need to inhibit CFTR by >90% to affect lung function. Our results thus support the further preclinical evaluation of small-molecule CFTR inhibitors as possible therapeutic agents to retard cyst growth in human ADPKD.

## CONCISE METHODS

### CFTR Inhibitors

For synthesis of tetrazolo-$CFTR_{inh}$-172 (compound T08, 3-[(3-trifluoromethyl)phenyl]-5-[(4-(1H-tetrazol-5-yl)phenyl)methylene]-2-thioxo-4-thiazolidinone), a mixture of 2-thioxo-3-(3-trifluoromethylphenyl)-4-thiazolidinone[16] (100 mg, 0.36 mmol) and 4-(1H-1,2,3,4-tetrazol-5-yl)benzaldehyde (63 mg, 0.36 mmol) in absolute alcohol (1 ml) containing piperidine (1 drop) was refluxed for 30 min. The yellow precipitate was filtered, washed with ethanol, dried, and recrystallized from ethanol to give 97 mg (62% yield) of a yellow powder. Melting point was from 146 to 149°C; ms ($ES^-$): M/Z 434 ($M^+$); $^1H$ NMR (400 MHz, DMSO-d6): 7.78 (d, 2H, carboxyphenyl,

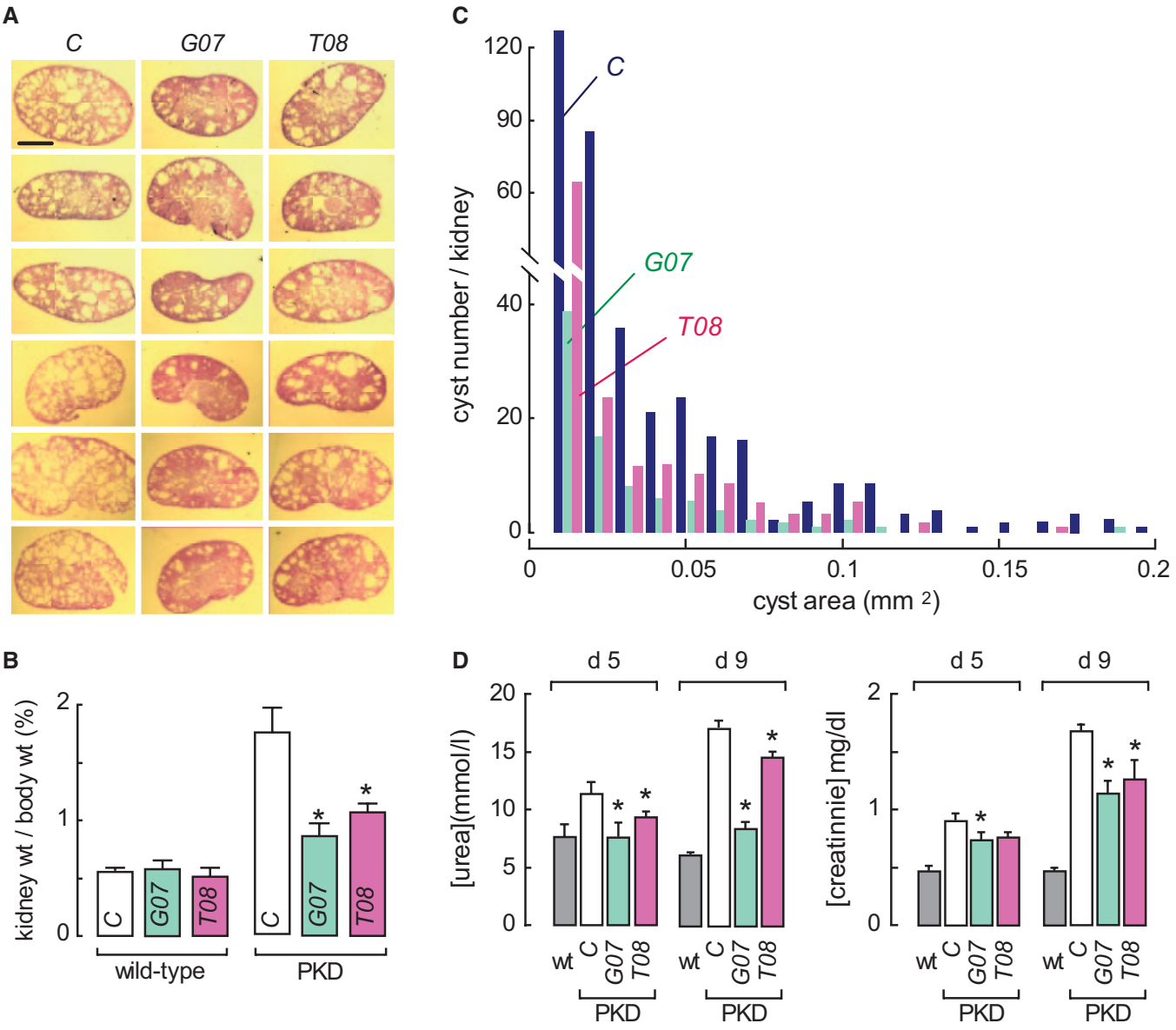


**Figure 7.** CFTR inhibitors slow cyst growth in a *Pkd1*$^{flox/-}$;*Ksp-Cre* mouse model of PKD. (A) Gallery of kidney sections from *Pkd1*$^{flox/-}$;*Ksp-Cre* mice treated for 3 d with DMSO vehicle (C, left) or CFTR inhibitors (5 to 10 mg/kg per d, middle and right). (B) Kidney weights (age 5 d) of non-PKD mice (denoted "wild-type") and *Pkd1*$^{flox/-}$;*Ksp-Cre* mice treated for 3 d with DMSO vehicle (C) or compounds T08 or G07 (SE, 11 mice per group, $*P < 0.01$). (C) Histogram of cyst numbers at indicated ranges of cyst areas (kidneys from 11 mice analyzed). (D) Renal function in CFTR inhibitor–treated *Pkd1*$^{flox/-}$;*Ksp-Cre* mice at ages 5 and 9 d. Mice were treated from day 2 onward. Serum creatinine and urea concentrations shown (SE, four mice per group, $*P < 0.05$ compared with control).

$J$ = 8.2 Hz), 7.80 to 8.00 (m, 5H, trifluoromethyl-phenyl and CH), 8.07 (d, 2H, carboxyphenyl, $J$ = 8.31 Hz), 13.20 (s, 1H, tetrazolo, $D_2O$ exchange).

For synthesis of Ph-GlyH-101 (compound G07, *N*-2-naphthalenyl-2-hydroxyethyl-[(3,5-dibromo-2,4-dihydroxyphenyl)methylene]-phenylglycinehydrazide), a mixture of 2-naphthylamine (0.72 g, 5 mmol), methyl α-bromophenylacetate (1.15 g, 5 mmol), and sodium acetate (0.82 g, 10 mmol) in 1 ml of water was stirred at 80°C for 5 h. The resultant solid after cooling was filtered and recrystallized from ethanol to yield 0.83 g of ethyl *N*-(2-naphthalenyl) glycinate (yield 57%, melting point 137 to 138°C). A solution of ethyl *N*-(2-naphthalenyl) glycinate (1.45 g, 5 mmol) in ethanol (10 ml) was refluxed with hydrazine hydrate (1 g, 20 mmol) for 6 h. Solvent and excess reagents were distilled under vacuum. The product was recrystallized from ethanol to yield 1.14 g of *N*-(2-naphthalenyl)-α-phenyl glycine hydrazide (78%, mp 176 to 178°C). A mixture of the hydrazide (2.9 g, 10 mmol) and 3,5-dibromo-4-hydroxy-benzaldehyde (2.8 g, 10 mmol) in ethanol (10 ml) was refluxed for 6 h. The hydrazide that crystallized upon cooling was filtered, washed with ethanol, and recrystallized from ethanol to give 3.64 g (yield 66%) of Ph-GlyH-101. Melting point was >280°C (decomposition); ms ($ES^-$): M/Z 554 ($M^+$); $^1H$ NMR (DMSO-$d_6$): δ 4.1 (s, 2H, CH), 6.5 to 7.5 (m, 14H,

aromatic, NH), 8.5 (s, 1H, CH = N), 10.4 (s, 1H, NH-CO), 11.9 (s, 1H, OH), 12.7 (s, 1H, OH). Synthesis procedures for compounds T01 through T07, T09 through T16, G01 through G06, and G08 through G16 were as described previously,[16,22,23] with minor variations.

## MDCK Model of Cyst Growth

Type I MDCK cells (ATCC No. CCL-34) were cultured at 37°C in a humidified 95% air/5% $CO_2$ atmosphere in a 1:1 mixture of DMEM and Ham's F-12 nutrient medium supplemented with 10% FBS (Hyclone, Logan, UT), 100 U/ml penicillin, and 100 $\mu$g/ml streptomycin. For generation of cysts, 400 MDCK cells were suspended in 0.4 ml of ice-cold Minimum Essential Medium containing 2.9 mg/ml collagen (PureCol; Inamed Biomaterials, Fremont CA), 10 mM HEPES, 27 mM $NaHCO_3$, 100 U/ml penicillin, and 100 $\mu$g/ml streptomycin (pH 7.4). The cell suspension was plated onto 24-well plates. After gel formation, 1.5 ml of MDCK cell medium containing 10 $\mu$M forskolin was added to each well, and plates were maintained at 37°C in a 5% $CO_2$ humidified atmosphere.

For testing CFTR inhibitors, compounds were included in the culture medium in the continued presence of forskolin from day 0 onward. Medium containing forskolin and test compounds was changed every 12 h. At day 6, cysts (with diameters >50 $\mu$m) and noncyst cell colonies were counted by phase-contrast light microscopy at ×20 magnification (546 nm monochromatic illumination) using a Nikon TE 2000-S inverted microscope (Nikon Corporation, Tokyo, Japan). In some experiments, compounds were added to medium in the continued presence of forskolin from day 4 after seeding, and the medium containing forskolin and compounds was changed every 12 h for 8 d. Micrographs showing the same cysts in collagen gels (identified by markings on plates) were obtained every 2 d. For determination of cyst growth, cyst diameters were measured using Image J software. At least 10 cysts per well and three wells per group were measured for each condition.

## Cytotoxicity, Cell Proliferation, and Apoptosis

Crystal violet staining[38] was used to assess compound effects on cytotoxicity. MDCK cells were incubated for 24 h on 96-well plates and then incubated for 72 h with test compounds at 20 $\mu$M. Medium was removed, and adherent cells were fixed and stained for 30 min with 0.5% crystal violet in 20% methanol. Plates were washed with distilled water, stain was extracted with Sorenson's buffer (0.1 mol/L sodium citrate [pH 4.2] in 50% ethanol) overnight at 4°C, and absorbance was measured at 570 nm. Cell proliferation was assayed using a bromodeoxyuridine (BrdU) cell proliferation assay kit (Calbiochem, San Diego, CA). MDCK cells ($10^4$/well) were seeded on 96-well plates and incubated for 72 h with test compounds at 5, 10, or 20 $\mu$M. BrdU was added at 60 h of culture. BrdU incorporation was measured according to the manufacturer's instructions by absorbance at 490 nm. Apoptosis was measured using the *in situ* cell death detection kit (Roche Diagnostics, Indianapolis, IN). MDCK cells were seeded on eight-chamber polystyrene tissue culture–treated glass slides and incubated with compounds T08 and G07 for 72 h at 5, 10, or 20 $\mu$M. For embryonic organ culture and *Pkd1*$^{flox/-}$*;Ksp-Cre* mouse models, paraffin-embedded tissue sections were dewaxed and rehydrated. Assay was done according to the manufacturer's instructions. Five microscopic fields were analyzed per condition. Apoptosis index was calculated as the percentage of nucleus-stained cells.

## Short-Circuit Current Measurements

Snapwell inserts containing MDCK cells (transepithelial resistance 1000 to 2000 Ohms) were mounted in a standard Ussing chamber system. The basolateral membrane was permeabilized with 250 $\mu$g/ml amphotericin B. The hemichambers were filled with 5 ml of 65 mM NaCl, 65 mM Na-gluconate, 2.7 mM KCl, 1.5 mM $KH_2PO_4$, 1 mM $CaCl_2$, 0.5 mM $MgCl_2$, Na-HEPES, and 10 mM glucose (apical) and with 130 mM NaCl, 2.7 mM KCl, 1.5 mM $KH_2PO_4$, 1 mM $CaCl_2$, 0.5 mM $MgCl_2$, Na-Hepes, and 10 mM glucose (basolateral; pH 7.3). Short-circuit current was recorded continuously using a DVC-1000 voltage clamp (World Precision Instruments, Sarasota, FL) with Ag/AgCl electrodes and 1 M KCl agar bridges.

In some experiments, MDCK cells in Snapwell inserts were cultured in medium containing 10 $\mu$M T08 or G07 for 1 or 48 h. Compounds were washed out with medium for 1 h before short-circuit current measurements.

## Embryonic Organ Culture Model

Mouse embryos were obtained at E13.5. Metanephroi were dissected and placed on transparent Falcon 0.4-$\mu$m-diameter porous cell culture inserts.[17] To the culture inserts was added DMEM/Ham's F-12 nutrient medium supplemented with 2 mM L-glutamine, 10 mM HEPES, 5 $\mu$g/ml insulin, 5 $\mu$g/ml transferrin, 2.8 nM selenium, 25 ng/ml prostaglandin E, 32 pg/ml T3, 250 U/ml penicillin, and 250 $\mu$g/ml streptomycin. Kidneys were maintained in a 37°C humidified $CO_2$ incubator for up to 6 d. Culture medium containing 100 $\mu$M 8-Br-cAMP, with or without CFTR inhibitors, was replaced (in the lower chamber) every 12 h. Kidneys were photographed using a Nikon inverted microscope (Nikon TE 2000-S) equipped with ×2 objective lens, 520-nm bandpass filter, and high-resolution PixeLINK color CCD camera. Cyst area was calculated as total cyst area divided by total kidney area.

## Pkd1/Ksp-Cre Mouse Model of ADPKD

*Pkd1*$^{flox}$ mice and *Ksp-Cre* transgenic mice in a C57BL/6 background were generated as described previously.[25,37] *Ksp-Cre* mice express Cre recombinase under the control of the Ksp-cadherin promoter.[37] *Pkd1*$^{flox/-}$*;Ksp-Cre* mice were generated by cross-breeding *Pkd1*$^{flox/flox}$ mice with *Pkd1*$^{+/-}$*:Ksp-Cre* mice.[25] Neonatal mice (age 1 d) were genotyped by genomic PCR.

CFTR inhibitors (5 to 10 mg/kg per d) or saline DMSO vehicle control (0.05 ml/injection) was administrated by subcutaneous injection on the back of neonatal mice four times a day for 3 or 7 d using a 1-ml insulin syringe, beginning at age 2 d (11 mice per group). *Pkd1*$^{flox/+}$*;Ksp-Cre* or *Pkd1*$^{flox/+}$ mice from the same litter were used as controls. Body weight was measured at day 5. Blood and urine samples were collected for measurement of CFTR inhibitor concentration and renal function. Kidneys were removed and weighed and fixed for histologic examination or homogenized for determination of CFTR inhibitor content.

### Histology

Kidneys were fixed with Bouin's fixative and embedded in paraffin. Three-micrometer-thick sections were cut serially every 200 $\mu$m and stained with hematoxylin and eosin. Sections were imaged using a Leica inverted epifluorescence microscope (DM 4000B, Wetzlar, Germany) equipped with $\times$2.5 objective lens and color CCD camera (Spot, model RT KE; Diagnostic Instruments, Sterling Heights, MI).

### Quantification of Cyst Growth

Cyst sizes in micrographs of metanephroi and kidney sections were determined using MATLAB 7.0 software (Natick, MA). A masking procedure was used to highlight all pixels of similar intensity within each cyst. Fractional cyst area was calculated as total cyst area divided by total kidney area. Cysts with diameters $>$50 $\mu$m were included in the analysis. Image acquisition and analysis were done without knowledge of treatment condition.

### Assay of Serum Creatinine and Urea

Serum was obtained from whole blood by centrifugation at 5000 $\times$ *g* for 5 min. Serum creatinine concentration was measured using a colorimetric assay kit (Cayman Chemical, Ann Arbor, MI) following the manufacturer's instructions. Urea concentration was measured using the colorimetric QuantiChrom Urea Assay Kit (BioAssay Systems, Hayward, CA). Creatinine and urea concentrations were determined from optical densities using calibration standards.

### HPLC/Mass Spectrometry

Kidneys were homogenized in 50 to 100 $\mu$l of PBS for 5 min using an Eppendorf pellet pestle homogenizer. The homogenate was mixed with an equal volume of chilled acetonitrile to precipitate proteins. After centrifugation at 5000 $\times$ *g* for 10 min, the supernatant was evaporated under nitrogen, and the residue was dissolved in eluent (50% $CH_3CN$/20 mM $NH_4OAc$). Urine samples were directly diluted 10-fold with eluent. Reversed-phase HPLC separations were carried out using a Waters C18 column (2.1 $\times$ 100 mm, 2.5-$\mu$m particle size) equipped with a solvent delivery system (Waters model 2690, Milford, MA). The solvent system consisted of a linear gradient from 20% $CH_3CN$/20 mM $NH_4OAc$ to 95% $CH_3CN$/20 mM $NH_4OAc$, run over 20 min, followed by 5 min at 95% $CH_3CN$/20 mM $NH_4OAc$ (0.2 ml/min flow rate). Mass spectra were acquired on an Alliance HT 2790 + ZQ mass spectrometer (Waters, Milford, MA) using negative ion detection, scanning from 150 to 1500 Da. The electrospray ion source parameters were as follows: Capillary voltage 3.2 kV (negative ion mode) or 3.5 kV (positive ion mode), cone voltage 37 V, source temperature 120°C, desolvation temperature 250°C, cone gas flow 25 L/h, and desolvation gas flow 350 L/h.

## ACKNOWLEDGMENTS

This study was supported by National Institutes of Health grants HL73856, DK72517, EB00415, HL59198, DK35124, and EY13574; Research Development Program and Drug Discovery grants from the Cystic Fibrosis Foundation (to A.S.V.), DK54053 and DK57328 (to S.S.); and Polycystic Kidney Disease Foundation grant 147a2r (to B.Y.).

We thank Peter Igarashi for the *Ksp-Cre* mouse strain. We thank Dr. Songwan Jin for help with image analysis and Liman Qian for mouse breeding.

## DISCLOSURES

None.

## REFERENCES

1. Arnaout MA: Molecular genetics and pathogenesis of autosomal dominant polycystic kidney disease. *Annu Rev Med* 52: 93–123, 2001
2. Gabow PA: Autosomal dominant polycystic kidney disease. *N Engl J Med* 329: 332–342, 1993
3. Harris PC, Rossetti S: Molecular genetics of autosomal recessive polycystic kidney disease. *Mol Genet Metab* 81: 75–85, 2004
4. Wilson P: Molecular and cellular aspects of polycystic kidney disease. *N Engl J Med* 350: 151–164, 2004
5. Sweeney WE Jr, Avner ED: Molecular and cellular pathophysiology of autosomal recessive polycystic kidney disease (ARPKD). *Cell Tissue Res* 326: 671–685, 2006
6. Chapman AB: Autosomal dominant polycystic kidney disease: Time for a change? *J Am Soc Nephrol* 18: 1399–1407, 2007
7. Qian F, Watnick TJ, Onuchic LF, Germino GG: The molecular basis of focal cyst formation in human autosomal dominant polycystic kidney disease type I. *Cell* 87: 979–987, 1996
8. Wu G, D'Agati V, Cai Y, Markowitz G, Park JH, Reynolds DM, Maeda Y, Le TC, Hou H Jr, Kucherlapati R, Edelmann W, Somlo S: Somatic inactivation of Pkd2 results in polycystic kidney disease. *Cell* 93: 177–188, 1998
9. Watnick TJ, He N, Wang K, Liang Y, Parfrey P, Hefferton D, St. George-Hyslop P, Germino GG, Pei Y: Mutations of *PKD1* in ADPKD2 cysts suggest a pathogenic effect of *trans*-heterozygous mutations. *Nat Genet* 25: 143–144, 2000
10. Torres VE, Wang X, Qian Q, Somlo S, Harris PC, Gattone VH 2nd: Effective treatment of an orthologous model of autosomal dominant polycystic kidney disease. *Nat Med* 10: 363–364, 2004
11. Ye M, Grantham JJ: The secretion of fluid by renal cysts from patients with autosomal dominant polycystic kidney disease. *N Engl J Med* 329: 310–313, 1993
12. Davidow CJ, Maser RL, Rome LA, Calvet JP, Grantham JJ: The cystic fibrosis transmembrane conductance regulator mediates transepithelial fluid secretion by human autosomal dominant polycystic kidney disease epithelium in vitro. *Kidney Int* 50: 208–218, 1996
13. Sullivan LP, Wallace DP, Grantham JJ: Epithelial transport in polycystic kidney disease. *Physiol Rev* 78: 1165–1191, 1998
14. Li H, Findlay IA, Sheppard DN: The relationship between cell proliferation, Cl− secretion, and renal cyst growth: A study using CFTR inhibitors. *Kidney Int* 66: 1926–1938, 2004
15. Brill SR, Ross KE, Davidow CJ, Ye M, Grantham JJ, Caplan MJ: Immunolocalization of ion transport proteins in human autosomal dominant polycystic kidney epithelial cells. *Proc Natl Acad Sci U S A* 93: 10206–10211, 1996
16. Ma T, Thiagarajah JR, Yang H, Sonawane ND, Folli C, Galietta LJ, Verkman AS: Thiazolidinone CFTR inhibitor identified by high-

throughput screening blocks cholera toxin-induced intestinal fluid secretion. *J Clin Invest* 110: 1651–1658, 2002
17. Magenheimer BS, St John PL, Isom KS, Abrahamson DR, De Lisle RC, Wallace DP, Maser RL, Grantham JJ, Calvet JP: Early embryonic renal tubules of wild-type and polycystic kidney disease kidneys respond to cAMP stimulation with cystic fibrosis transmembrane conductance regulator/Na+,K+,2Cl− co-transporter-dependent cystic dilation. *J Am Soc Nephrol* 17: 3424–3437, 2006
18. O'Sullivan DA, Torres VE, Gabow PA, Thibodeau SN, King BF, Bergstralh EJ: Cystic fibrosis and the phenotypic expression of autosomal dominant polycystic kidney disease. *Am J Kidney Dis* 32: 976–983, 1998
19. Xu N, Glockner JF, Rossetti S, Babovich-Vuksanovic D, Harris PC, Torres VE: Autosomal dominant polycystic kidney disease coexisting with cystic fibrosis. *J Nephrol* 19: 529–534, 2006
20. Taddei A, Folli C, Zegarra-Moran O, Fanen P, Verkman AS, Galietta LJ: Altered channel gating mechanism for CFTR inhibition by a high-affinity thiazolidinone blocker. *FEBS Lett* 558: 52–56, 2004
21. Sonawane ND, Muanprasat C, Nagatani R, Song Y, Verkman AS: In vivo pharmacology and antidiarrheal efficacy of a thiazolidinone CFTR inhibitor in rodents. *J Pharm Sci* 94: 134–143, 2004
22. Muanprasat C, Sonawane ND, Salinas D, Taddei A, Galietta LJ, Verkman AS: Discovery of glycine hydrazide pore-occluding CFTR inhibitors: Mechanism, structure-activity analysis, and in vivo efficacy. *J Gen Physiol* 124: 125–137, 2004
23. Sonawane ND, Hu J, Muanprasat C, Verkman AS: Luminally active, nonabsorbable CFTR inhibitors as potential therapy to reduce intestinal fluid loss in cholera. *FASEB J* 20: 130–132, 2006
24. Sonawane ND, Zhao D, Zegarra-Moran O, Galietta LJ, Verkman AS: Lectin conjugates as potent, nonabsorbable CFTR inhibitors for reducing intestinal fluid secretion in cholera. *Gastroenterology* 132: 1234–1244, 2007
25. Shibazaki S, Yu Z, Nishio S, Tian X, Thomson RB, Mitobe M, Louvi A, Velazquez H, Ishibe S, Cantley LG, Igarashi P, Somlo S: Cyst formation and activation of the extracellular regulated kinase pathway after kidney specific inactivation of Pkd1. *Hum Mol Genet* 2008 Feb 7 [Epub ahead of print]
26. Mangoo-Karim R, Uchic ME, Grant M, Shumate WA, Calvet JP, Park CH, Grantham JJ: Renal epithelial fluid secretion and cyst growth: The role of cyclic AMP. *FASEB J* 3: 2629–2632, 1989
27. Mangoo-Karim R, Uchic M, Lechene C, Grantham JJ: Renal epithelial cyst formation and enlargement in vitro: Dependence on cAMP. *Proc Natl Acad Sci U S A* 86: 6007–6011, 1989
28. Grantham JJ, Mangoo-Karim R, Uchic ME, Grant M, Shumate WA, Park CH, Calvet JP: Net fluid secretion by mammalian renal epithelial cells: Stimulation by cAMP in polarized cultures derived from established renal cells and from normal and polycystic kidneys. *Trans Assoc Am Physicians* 102: 158–162, 1989
29. Murcia NS, Sweeney WE Jr, Avner ED: New insights into the molecular pathophysiology of polycystic kidney disease. *Kidney Int* 55: 1187–1197, 1999
30. Igarashi P, Somlo S: Genetics and pathogenesis of polycystic kidney disease. *J Am Soc Nephrol* 13: 2384–2388, 2002
31. Tanner GA, McQuillan PF, Maxwell MR, Keck JK, McAteer JA: An in vitro test of the cell stretch-proliferation hypothesis of renal cyst enlargement. *J Am Soc Nephrol* 6: 1230–1341, 1995
32. Mohamed A, Ferguson D, Seibert FS, Cai HM, Kartner N, Grinstein S, Riordan JR, Lukacs GL: Functional expression and apical localization of the cystic fibrosis transmembrane conductance regulator in MDCK I cells. *Biochem J* 322: 259–265, 1997
33. McAteer JA, Dougherty GS, Gardner KD Jr, Evan AP: Scanning electron microscopy of kidney cells in culture: Surface features of polarized epithelia. *Scan Electron Microsc* (Pt 3): 1135–1150, 1986
34. McAteer JA, Dougherty GS, Gardner KD, Evan AP: Polarized epithelial cysts in vitro: a review of cell and explant culture systems that exhibit epithelial cyst formation. *Scanning Microsc* 2: 1739–1763, 1988
35. Taide M, Kanda S, Igawa T, Eguchi J, Kanetake H, Saito Y: Human simple renal cyst fluid contains a cyst formation-promoting activity for Madin-Darby canine kidney cells cultured in collagen gel. *Eur J Clin Invest* 26: 506–513, 1996
36. Gupta IR, Lapointe M, Yu OH: Morphogenesis during mouse embryonic kidney explant culture. *Kidney Int* 63: 365–376, 2003
37. Shao X, Somlo S, Igarashi P: Epithelial-specific Cre/lox recombination in the developing kidney and genitourinary tract. *J Am Soc Nephrol* 13: 1837–1846, 2002
38. Johnson FM, Saigal B, Talpaz M, Donato NJ: Dasatinib (BMS-354825) tyrosine kinase inhibitor suppresses invasion and induces cell cycle arrest and apoptosis of head and neck squamous cell carcinoma and non-small cell lung cancer cells. *Clin Cancer Res* 11: 6924–6932, 2005